frontiers in Physics

REVIEW
published: 10 February 2021
doi: 10.3389/fphy.2020.580602

Recent Advance in Tunable Single-Frequency Fiber Laser Based on Two-Dimensional Materials

Zhe Wei[1,2], *Shuangcheng Chen*[1,2], *Jianyi Ding*[1,2], *Bo Sun*[1,2], *Xinyuan Qi*[3]*, *Baole Lu*[1,2]* and *Jintao Bai*[1,2]

[1]Key Laboratory of Photoelectric Technology and Functional Materials, International Collaborative Center on Photoelectric Technology and Nano Functional Materials, Institute of Photonics and Photon-technology, Northwest University, Xi'an, China, [2]Shaanxi Engineering Technology Research Center for Solid State Lasers and Application, Provincial Key Laboratory of Photoelectronic Technology, Northwest University, Xi'an, China, [3]School of Physics, Northwest University, Xi'an, China

Two-dimensional (2D) materials possess optoelectronic and nonlinear optical properties make them used in many fields such as optical modulator, optical switch, and single frequency (SF) fiber lasers as a saturable absorber (SA) in the laser cavity. This review deals with recent advances in wavelength tunable single frequency fiber laser based on these properties. It extends the contents from previous reviews on pulsed fiber lasers to SF fiber lasers which have emerged in recent years. First, the research status of 2D materials, including the structural characteristics and properties of some typical cases and their saturable absorption characteristics are introduced. After that, the principle and some applicable technologies with these 2D materials to achieve the wavelength tunable SF operation are discussed. Further, the latest research progress on such fiber lasers are summarized. Finally, a discussion on future prospects and challenges are included.

Keywords: single-frequency, fiber laser, two-dimensional materials, tunable wavelength, narrow linewidth, saturable absorber

OPEN ACCESS

Edited by:
Xinping Zhang,
Beijing University of Technology, China

Reviewed by:
Han Zhang,
Shenzhen University, China
Chujun Zhao,
Hunan University, China

***Correspondence:**
Xinyuan Qi
qixycn@foxmail.com
Baole Lu
lubaole1123@163.com

Specialty section:
This article was submitted to Optics and Photonics, a section of the journal Frontiers in Physics

Received: *06 July 2020*
Accepted: *22 September 2020*
Published: *10 February 2021*

Citation:
Wei Z, Chen S, Ding J, Sun B, Qi X, Lu B and Bai J (2021) Recent Advance in Tunable Single-Frequency Fiber Laser Based on Two-Dimensional Materials. Front. Phys. 8:580602. doi: 10.3389/fphy.2020.580602

INTRODUCTION

In recent year, 2D layered materials have made rapid development after the discovery of grapheme. Graphene, as the first 2D material have thermal transport, optical properties, and electronic transport. After the studies of grapheme, a series of 2D layers materials such as black phosphorus, metal chalcogenide compounds, transition metal oxides and other 2D compounds materials have attracted research interests because of high performance in optoelectronic and nonlinear optical properties, which make them as a saturable absorber (SA) in laser cavity. The common feature of 2D layered materials is the massive three-dimensional crystal stack structure [1]. There is a van der Waals interaction force between adjacent sheets, and each sheet has a strong covalent bond. This material spans all electronic structures from insulators to metals and shows special characteristics, including topological insulator effect, superconductivity and thermoelectricity.

Fiber laser, which combine 2D materials with optical fibers, optical resonant cavities, and optical waveguides, have achieved breakthroughs in recent years. Many achievements have been made in the research direction of laser pulse light generation, single-frequency (SF) laser and other lasers using the 2D material, due to its advantages of narrow linewidth, excellent monochromaticity, high coherence, low noise and compact structure, SF fiber lasers are widely used in high-frequency resolution spectroscopy, coherent lidar, gravity wave detection, material micromachining and

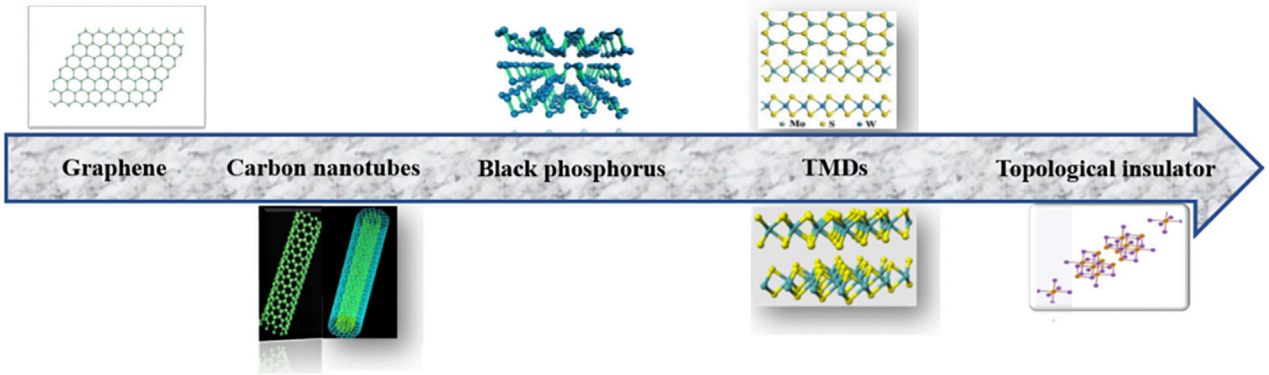

FIGURE 1 | Low-dimensional material crystal structure.

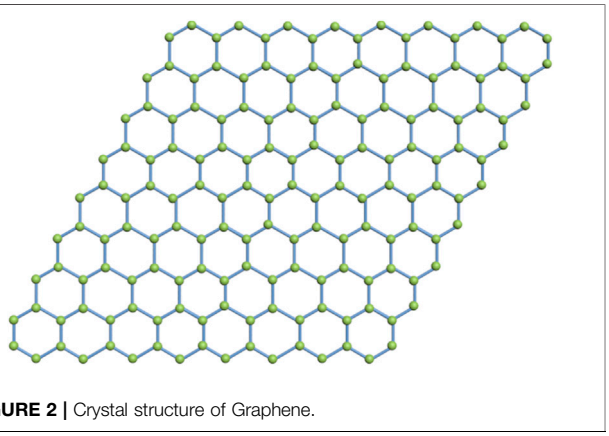

FIGURE 2 | Crystal structure of Graphene.

precision measurement [2–4] and have become one of the most promising research fields in the laser field. The SF Q-switched fiber laser has the characteristics of narrow line width and high coherence, and can further compress the pulse width and increase the beam power. This has great potential for applications in spaceborne lidar and space laser communications. Therefore, the research of SF Q-switched lasers is of great significance to promote its application range and enhance its application value [5–10].

The development and research of tunable single longitudinal mode fiber lasers based on two-dimensional materials has continued for many years. Single-frequency fiber lasers have the characteristics of wide, low noise and compact structure, and are widely used in fiber sensing, optical communication, microwave generation and high-resolution spectroscopy [16, 32, 36, 40, 48, 56, 77, 78, 98]. **Figure 1** shows the crystal structure of various low-dimensional materials. Their common feature is the layered molecular structure.

This article will discuss in detail from the aspects of 2D material structure characteristics, saturable absorption characteristics and the application of 2D materials in SF fiber lasers. Make a corresponding categorization summary of the relationship between material characterization and saturable absorption characteristics.

2D MATERIAL STRUCTURAL CHARACTERISTICS AND PROPERTIES

Graphene

Graphene has a Dirac gapless structure and its unique linear energy momentum dispersion relationship is:

$$E\left(k_x, k_y\right) = \pm \gamma_0 \sqrt{1 + 4\cos\frac{\sqrt{3}k_x a}{2}\cos\frac{k_y a}{2} + 4cos^2\frac{k_y a}{2}} \quad (1)$$

In **Eq. 1**, k_x and k_y are the x, y components of the wave vector k, ± 1 represents the conduction band and valence band, and γ_0 represents the energy barrier that the valence electron must overcome to transition between two adjacent carbon atoms as (2.9–3.1eV), $a = 3^{0.5}a$ ($a = 0.142$ nm). The carbon atom contains π electron, so the valence band of graphene is in the full state and the conduction band is in the empty state, and its Fermi surface is at the Dirac point. Therefore, graphene is a zero-band gap semiconductor material in the theoretical model.

Due to the unique crystal structure of grapheme, as shown in **Figure 2**, it has special properties, various material properties are produced. Graphene has a unique energy band structure and has light absorption characteristics in ultraviolet light, even terahertz and microwave bands, and a single layer of graphene can absorb 2.3% of visible light and incident light in the near infrared band, as shown in **Figure 3**. It is worth noting that the Fermi level of graphene can be adjusted by electrical gating and chemical doping. This feature allows us to precisely modulate the optical properties of graphene in the visible and infrared bands. In addition, graphene exhibits ultrafast carrier dynamics, high carrier mobility, wavelength-independent absorption, tunable optical properties, and strong electromagnetic field localization. Graphene also exhibits strong nonlinear optical properties [19], with high third-order susceptibility in the visible and near-infrared bands. Due to the strong covalent bonding between atoms, graphene has excellent stability and mechanical properties. All these characteristics of graphene make it have important application value in broadband tunable devices.

Black Phosphorus

Black phosphorus (BP) is another kind of direct band gap semiconductor. Due to BP special layered structure, the band gap can be adjusted by changing the number of layers as shown in **Figure 4**. The band gap of BP will increase as the number of layers decreases. The single-layer BP band gap is 2 eV, which fills the zero band. The gap between the gap graphene and the wider-band gap transition metal sulfide can be used for light detection, light modulation, and even biophotonics. Due to the anisotropy of BP, in-plane electrical conductivity and photoconductivity are also anisotropic, resulting in highly anisotropic light absorption and photoluminescence.

Transition Metal Dichalcogenides

In addition to graphene, transition metal dichalcogenides (TMDs) have also been extensively studied, and its chemical formula is MX_2 (M = Mo, W, Re; X = S, Se, Te). Since single-layer metal sulfides are usually semiconductor materials, their optical properties are different from graphene, and their application fields are more extensive and complementary. The bandgap coverage range is 1–2.5 eV, and the corresponding spectral range is visible light to near infrared. One of the important characteristics of transition metal sulfides is that with the thickness of the material from multilayer to single layer, the transition metal sulfur transitions from an indirect band gap to a direct band gap, such as MoS_2, $MoSe_2$, WS_2, and WSe_2 are indirect bands in the bulk Gap semiconductor form, but in a single layer, its band gap becomes a direct band gap. In addition, a single layer of transition metal sulfide material can achieve 20% absorption of specific resonance energy. These characteristics are conducive to the generation of mode-locked lasers, nonlinear optics, and harmonics.

Other Two-Dimensional Materials

Because of the excellent optical properties and material properties of 2D materials, the types of research on 2D materials have exceeded these basic types. For example, topological insulators, various heterojunction 2D materials, and even liquid materials have optical properties similar to 2D materials.

Topological insulator is a state of matter with quantum characteristics, and its quantum characteristics are relatively novel. According to the band theory, solid materials can be divided into insulators, conductors and semiconductors according to their electrical conductivity. The different Fermi energy levels of the three materials show different material properties. Insulator materials have a finite energy gap at the Fermi level, so there are no free carriers; conductor materials have a finite electronic state density at the Fermi level, so they have free carriers; semiconductor materials are at the Fermi level There is no energy gap, but the density of electron states at the Fermi level is still zero. But topological insulators are similar to insulators, but not exactly the same. Theoretical analysis is carried out on the energy band structure. The energy band structure of this type of material belongs to the insulator type, and there is an energy gap at the Fermi energy. However, on the surface of this type of material, there is always a Dirac type that passes through the energy gap. The electronic state, thus causing its surface to always be metallic. The special electronic structure of the topological insulator is determined by the special topological properties of its band structure.

The characteristic of the 2D material is closely related with the manufacturing process. The different manufacturing processes directly effect the characteristics of the 2D material. Therefore, a series of detect methods are required to characterize the prepared 2D material samples after the production and ensured that the 2D material samples qualities to use. The main production processes of 2D materials are mechanical stripping method, liquid phase stripping method, chemical vapor deposition method, redox method, photo deposition method and pulse laser deposition method. After the preparation of the 2D material is completed, it is generally necessary to use various detection methods to characterize the material. At present, the characterization methods for 2D materials mainly include electron microscope, atomic force microscope, Raman spectrometer, XRD (X-ray diffraction) and nonlinear saturation absorption characteristic measurement.

Different applications have different requirements for 2D materials. In order to meet the needs of applications, we need to prepare 2D materials with different specifications. This requires that many factors must be considered at the same time, such as the thickness of the two material sheets. The size of the nanodevices and the purity of the materials, etc., it is necessary to explore methods that can easily and effectively prepare and characterize the detection of 2D materials. The following will introduce several common preparation methods.

TWO-DIMENSIONAL MATERIAL PREPARATION AND CHARACTERIZATION

Mechanical Exfoliation Method

The van der Waals force exists between the two-dimensional material crystal layered structure, so the van der Waals force in the layered structure can be destroyed by external force to obtain a single layer of two-dimensional material. As shown in **Figure 5**, using tape to pick up from the bulk material, and then repeat between tapes, and finally obtain a high-purity two-dimensional material. The mechanical peeling method does not destroy the covalent bond between the material layers, and the raw material used is a high-purity bulk material, so the resulting product has extremely high purity. Graphene was originally obtained by mechanical peeling. Since then, it has been widely used in the preparation of layered materials, such as black phosphorus, MoS2, Bi2Te3, and ReS2.

Liquid Phase Exfoliation Method

The principle of the liquid phase stripping method is to use the microwave shear force and thermal stress to destroy the van der Waals force between the material layers, and then mix with a specific auxiliary dispersant, such as N-methylpyrrolidone or N, H-dimethylformamide, etc. The material is peeled off layer by layer. The general operation flow is shown in **Figure 6**. First, the powdered material and the stripping solution are mixed in proportion. The stripping solution is generally an organic

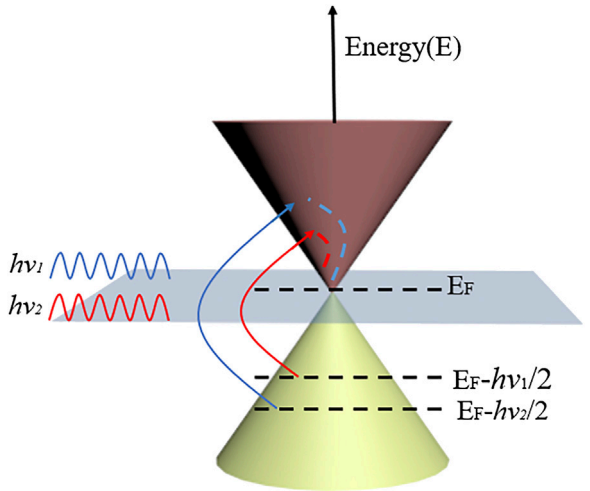

FIGURE 3 | Diagram of graphene's band structure and photon absorption.

solvent such as N-methyl pyrrolidone or N, H-dimethylformamide. Put the mixed liquid into the ultrasonic crusher for water bath heating treatment, and choose different crushing time according to different materials. After the ultrasonic treatment, the mixed liquid is loaded into a centrifuge tube and centrifuged. After the centrifugation process is completed, the solution is layered, and the supernatant is extracted for vacuum suction filtration, and a layer of material film is covered on the filter paper. The concentration of the solution can be changed to adjust the thickness of the material. After removing the filter paper with an organic solvent, a complete two-dimensional material sheet is obtained, which is placed in a vacuum drying box for storage and drying. Or directly use the supernatant after the centrifugation is completed for the experiment.

The materials prepared by the liquid-phase stripping method include carbon nanotubes, black phosphorus, WS2, BeTi2, etc. The liquid-phase stripping has wide applicability to the materials, the preparation process is simple, the efficiency is high, and the experimental requirements are low. However, the solvent requirements are higher.

Chemical Vapor Deposition

Chemical vapor deposition (CVD) is a process technology in which a reactive substance undergoes a chemical reaction under relatively high temperature and gaseous conditions, and the resulting solid substance is deposited on the surface of a heated solid substrate, and then a solid material is produced. A gaseous mass transfer process that essentially belongs to the category of atoms. During the preparation of graphene [20, 21], methane or ethanol droplets are used as the carbon source, and Ar is used as the protective gas, so that the carbon source is introduced into the surface of the metal substrate in a gaseous manner. After a period of reaction, the carbon source is on the metal substrate. The graphene is decomposed and deposited in different layers, and finally the graphene and the substrate are separated by chemical etching to obtain graphene products. Carbon nanotubes [22, 23] are usually generated by cracking carbon-containing gas or liquid carbon source under the action of a catalyst at a certain temperature, so this method is also called catalytic cracking method. The catalyst is generally a transition metal (such as Fe, Co, Ni, Pd, etc.), and the carbon source can be carbon-containing gas such as methane, CO, ethylene, or liquid such as benzene and toluene.

Electric Arc Discharge Technology

This method was first applied to carbon nanotubes [24, 25]. It mainly uses transition metal or oxide as catalyst and graphite as electrode. In an inert gas environment, the arc graphite electrode is consumed by evaporation, and carbon nanotubes are deposited on the cathode graphite electrode.

Pulsed Laser Deposition Technology

Pulsed laser deposition (PLD) is a vacuum physical deposition process. The bulk material is usually used as the target material, and then graphene/copper and SiO2/Si are used as the substrate material. The pulsed light is focused on the surface of the target material, causing it to generate high temperature and ablation, thereby generating high temperature and pressure plasma. The plasma is oriented to expand and deposit on the substrate to form a thin film. Material thickness can be roughly controlled by laser pulses.

Magnetron Sputtering Deposition Method

The working principle of magnetron sputtering is that electrons collide with argon atoms in the process of flying to the substrate under the action of electric field *E*, which ionizes to produce Ar positive ions and new electrons. The new electrons flew to the substrate, Ar ions accelerated to the cathode target under the action of the electric field, and bombarded the target surface with high energy to cause the target to sputter. In sputtered particles, neutral target atoms or molecules are deposited on the substrate to form a thin film. General metal compounds will use this kind of manufacturing process to synthesize thin films, such as $MoTe_2$ [26], WTe_2 [27], MoS_2-WS_2 [28], etc.

Chemical Combination

Bi2Te3 nanosheets [29] were synthesized by diethylene glycol (DEG)-mediated polyol method. In a typical synthesis,

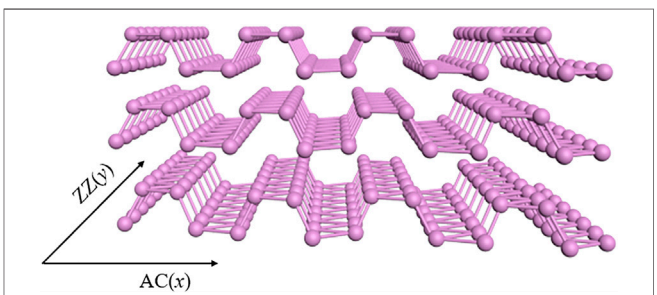

FIGURE 4 | Schematic diagram of layered BP, where the *x*-axis and *y*-axis are along the armchair (AC) and zigzag (ZZ) directions respectively.

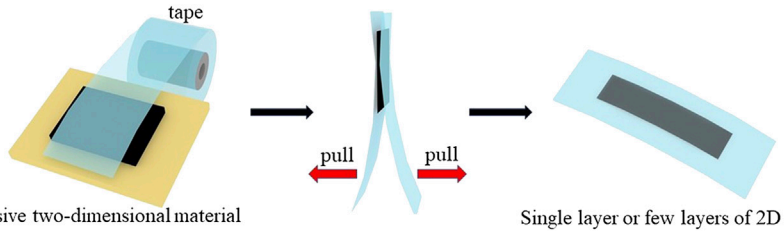

FIGURE 5 | Flow chart of two-dimensional material mechanical exfoliation method.

stoichiometric bismuth nitrate (Bi (NO_3)) and potassium telluride (K_2TeO_3) are dissolved in DEG and vigorously stirred, and then the mixed solution is refluxed at 240°C for 4–5 h. Then, the mixture was cooled to room temperature. The gray powder was collected by filtration, washed with distilled water and ethanol, and finally dried under vacuum at 60°C overnight. The powder after growth and washing is dispersed in an ethanol solution.

After the preparation of the two-dimensional material film is completed, a series of detection methods need to be used for detection. The crystal structure and phase composition of the film were analyzed by X-ray diffractometer (XRD), the surface and cross-sectional morphology of the film were observed by scanning electron microscope (SEM), and the physical properties and number of layers of the two-dimensional layered material were quickly characterized by Raman spectrometer (Raman).

SATURABLE ABSORPTION CHARACTERISTICS OF 2D MATERIALS

Single-frequency fiber lasers select and limit the number of longitudinal modes that vibrate in the resonator by adding a narrowband filter in the resonator, and only allow single-longitudinal, single-transverse, and single-polarization laser modes to generate stimulated amplification and final output. Two-dimensional materials can be used to make new filter components for pattern filtering. Most layered materials, such as graphene, topological insulators, and black phosphorus, have a symmetrical cone-shaped band structure. Physically, when the intensity of incident light is greater than the band gap of the layered material, any electrons can be excited into the conduction band. Then, the distribution rapidly heats and cools, forming a hot Fermi Dirac distribution. Through a dynamic process, the electron accelerator and holes recombine until the equilibrium distribution is restored. The linear optical transition at low excitation intensity is described. However, as the light intensity increases, the number of photocarriers increases rapidly, filling the energy states near the edges of the conduction band and the valence band. Due to the Poly blocking principle, absorption is blocked. Finally, photons of a specific wavelength can be transparently transmitted to the layered material without being absorbed, thereby achieving the effect of narrowing the line width [30]. In addition, 2D materials have very excellent thermal conductivity. The thermal conductivity of pure defect-free single-layer graphene is as high as 5300 W/mK, which is the carbon material with the highest thermal conductivity so far, higher than single-wall carbon nanotubes (3500 W/mK) and multi-wall carbon nanotubes (3000 W/mK). When it is used as a carrier, the thermal conductivity can also reach 600 W/mK. It is a novel idea to use the characteristics of two-dimensional materials to make tuning devices for center wavelength conversion [31].

Based on such characteristics of 2D materials, it has realized in 1, 1.5, and 2 μm pulsed fiber lasers. When the pulse laser passes through the SA, due to the nonlinear saturable absorption characteristics of the SA, the absorber will greatly absorb light with weaker light intensity and weaker with stronger light. When the edge part of the optical pulse passes through the SA, the transmittance is low and the loss is large, while the peak part of the pulse is large and the loss is low. The loss can be compensated by the amplification of the laser working substance. Therefore, when the light pulse circulates once in the cavity, the relative value of the intensity of the light signal will change once. When the optical signal in the cavity passes through multiple cycles, the energy difference between the peak value and the edge of the pulse will become larger and larger, the pulse will be continuously compressed and optical pulse is narrowed in the process of passing through the absorber, finally achieve the generation of pulsed laser.

The detection device of the saturable absorption characteristics of the 2D material in the fiber laser is shown in **Figure 7**. Using this device diagram, the nonlinear absorption characteristic data of the 2D material can be obtained, thereby obtaining the modulation depth of the 2D material. **Equation 2** is as follow:

$$a(I) = \frac{a_s}{1 + I/I_{sat}} + a_{ns} \tag{2}$$

where a_s is the modulation depth, a_{ns} is the unsaturated loss, and I_{sat} is the saturation absorption intensity [32].

The combination method of 2D material saturable absorption depicted in **Figure 8** is generally adopted. **Figure 8** shows a combination method of combining materials with a laser cavity. The material may be deposited on the glass plate as shown in **Figure 8A**, on the end face of the optical fiber connector as shown in **Figure 8B**, on the tapered fiber as shown in **Figure 8C** or on the

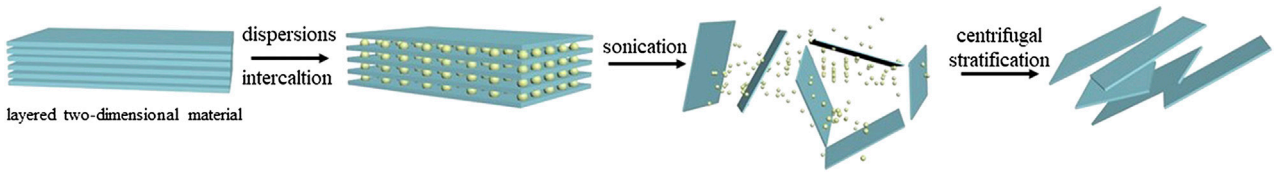

FIGURE 6 | Liquid phase exfoliation.

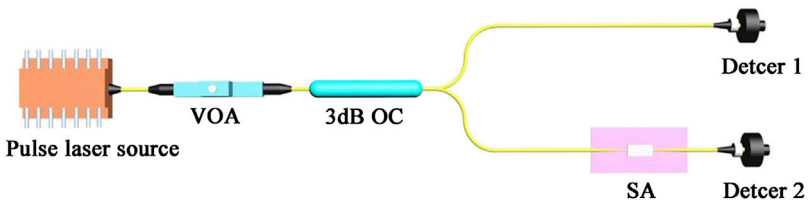

FIGURE 7 | Experimental device for measuring nonlinear saturation absorption characteristics.

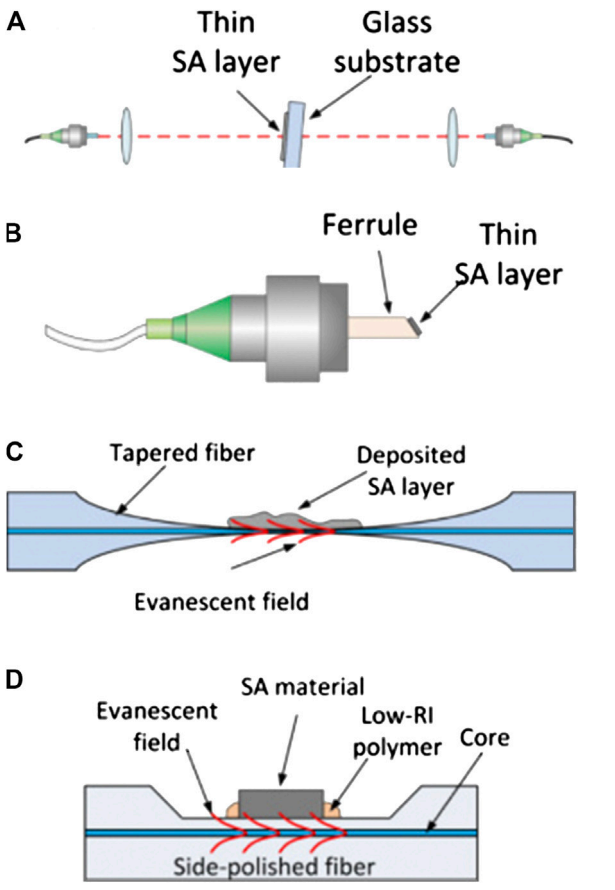

FIGURE 8 | Different types of SAs based on nanomaterials: **(A)** deposited on a glass plate, **(B)** on the end of the fiber connector, **(C)** on a tapered fiber, **(D)** on a side polished fiber (RI Refractive index).

side polished fiber surface as shown in **Figure 8D**. According to the manufacturing process and shape characteristics of the low-dimensional material, it is necessary to select the proper combination with the resonant cavity to achieve the best match.

The wide absorption spectrum range, photothermal effect and nonlinear absorption of 2D materials have made great achievements in the direction of pulsed light generation of fiber lasers. As show in **Table 1**. The use of 2D materials as optical modulation devices in SF fiber lasers has recently become one of research focuses. Therefore, this article focuses on discuss the recent representative research results of 2D materials in SF fiber lasers.

TUNABLE FIBER LASER BASED ON 2D MATERIAL

Tunable fiber lasers have attracted scholars due to their unique advantages and excellent performance, such as wide gain bandwidth, high stability, spectral purity, extremely narrow linewidth, wide tunable range and precise wavelength adjustment [41–55]. Reekie and his team studied tunable single-mode fiber lasers in 1980. However, most techniques are difficult to achieve wide-wavelength tuning [56–59], and some methods are unstable [60–66]. The working substance has a wide fluorescence spectrum in the laser, and it has the tunability in a certain wavelength range. Currently, there are three methods for implementing tunable fiber lasers. First, the wavelength corresponding to the low-loss region of the resonant cavity is controlled by the grating to change the center wavelength of the lasing. Second, the energy level of the laser transition is moved by changing parameters such as temperature and magnetic field. The last one is the use of nonlinear effects to achieve wavelength conversion and tuning. Typical tunable fiber lasers include temperature tuned fiber

TABLE 1 | Research progress of narrow-linewidth single-frequency pulsed fiber lasers based on low-dimensional materials.

Sas	Gain length (cm)	Center wavelength (nm)	Maximum power (mW)	Pulse duration (us)	Linewidth (kHz)	OSNR (dB)
MoS2 [33]	16	1,064	15.3	\	5.89	60
Ti: Bi2Te3 [34]	100	1,542.37–1,543.16	23	\	10	\
Graphene [35]	6	1,544.5	20	1–7	Sub-MHz	20
Graphene [36]	SOA	1,544.66, 1,545.36	18.2, 67.6	\	<7.3	50
Graphene [37]	100	1,547.88–1,559.88	214	\	206.25	66.0–68.3
Ni-MOF [38]	\	1,549.9	53	\	3.2	52
Bi2Se3 [39]	240	1,550.50	797,000	2.54	212	62
SWCNTs [40]	300	1,525–1,561	6.9	1.1–8.1	17.5	\

SOA, semiconductor optical amplifier; SWCNTs, single wall carbon nanotubes.

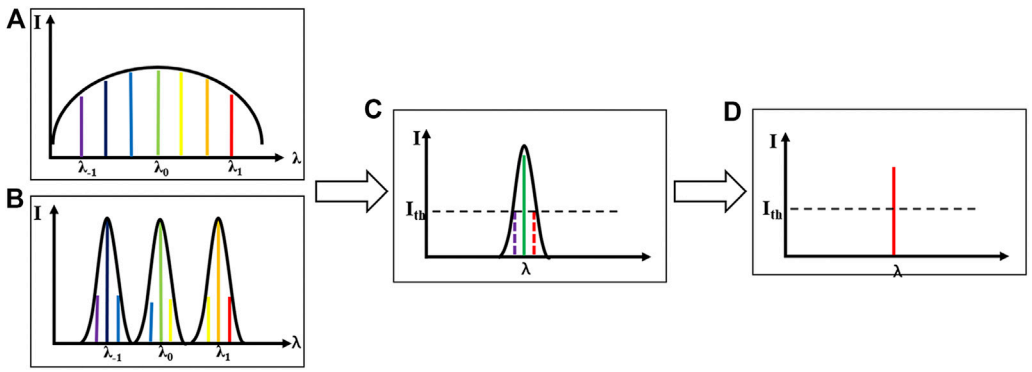

FIGURE 9 | (A) shows the broadband absorption characteristics of the saturated absorber, **(B)** shows the narrow line width through the filter, **(C)** shows the nonlinear effect of the saturated absorber, **(D)** single-frequency light output.

grating lasers and stress tuned fiber lasers. In recent years, 2D materials have been widely used in lasers, and tunable single-frequency lasers based on 2D materials have developed rapidly.

Principle of Tunable Single Frequency Fiber Laser

Traditional single-frequency fiber lasers are divided into short-line cavity and ring cavity. There are several common technical methods to realize single-frequency fiber lasers by using polarization incoherent technology, saturable absorber devices, and ultra-short linear cavity structures. In addition to using Rayleigh scattering, Raman scattering, stimulated Brillouin scattering, etc. Non-linear effects to achieve single-frequency operation methods are constantly reported [67–70]. The research on single-frequency fiber lasers first started in 1986. Jauncey et al. used neodymium-doped single-mode fiber as a gain medium and FBG as an end mirror to produce a laser output with a linewidth of 19 GHz and a center wavelength of 1,084 nm. Then in 1990, Iwatsuki and others successfully measured an ultra-narrow linewidth of 1.4 KHz based on the polarization maintaining technology with a circular cavity structure using a 72 km delay fiber [71]. In the following year, Ball et al. developed the 1,548 nm erbium-doped communication band Research on the narrow linewidth of fiber lasers and successfully developed a single-frequency output of 47 KHz [72]. In the following decades, it became one of the most promising research directions in the laser field [73–87].

Recently, the emergence of two-dimensional materials has attracted the attention of single-frequency fiber lasers. Scholars believe that introducing two-dimensional materials devices into fiber lasers has a good prospect. Since graphene was successfully discovered in 2004, it has become the most attractive research object for a time, due to graphene ultra-high stability [88], excellent electrical properties [89] and optical properties [90]. Because of its unique gapless structure, graphene absorption is only related to the light transmission constant and does not depend on the optical frequency [91], high mobility, good optical transparency and linear dispersion effect of Dirac electrons, so it has ultra-broadband Tunability [92]. As shown in **Figure 9**, graphene has unique broadband absorption characteristics. Therefore, graphene has attractive prospects in the field of ultra-wide bandwidth tuning. Since graphene has broadband absorption characteristics, the optical tuning device based on the two-dimensional material graphene does not need to consider the influence of wavelength, and has the advantages of good tuning accuracy and fast response speed. The zero band gap system of graphene. The structure can generate heat by absorbing photons to generate phonon relaxation oscillations. With its thermal conductivity of 5,300 W/mK, graphene can quickly transfer the Joule heat generated by the photothermal effect, and can easily generate controllable light with

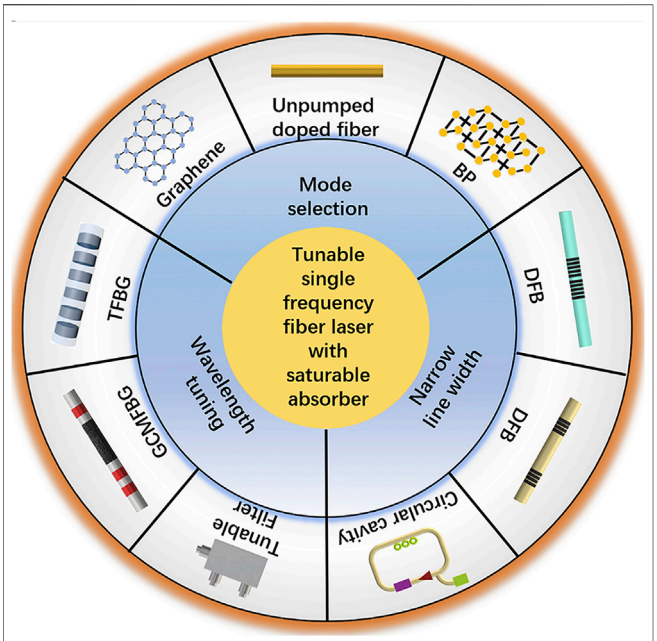

FIGURE 10 | The main technology of tunable single frequency fiber laser.

a response time of microseconds. Thermal conversion [93]. **Figure 10** shows some fiber laser functional devices.

Latest Research Progress

Harith Ahmad et al. reported a SLM tunable fiber laser based on graphene SA to generate radio frequency (microwave) signals [94]. Using index matching gel (IMG) to obtain ferrules for graphene deposition, which is simpler than traditional optical and chemical phase deposition methods. The SLM output is mixed with another output signal from a tunable laser source (TLS) to form a radio frequency (RF) signal. Tunable SLM fiber ring laser uses a length of 1 m of highly doped fiber as the gain medium in this experiment. In the past, such experiments usually used a section of unpumped doped fiber to generate the SLM output. This work used a novel graphene saturation absorber to generate the SLM output. The tunable fiber grating determines the tuning range of the fiber ring laser, and the tunable range is 1,547.88–1,559.88 nm.

Graphene has unique optical properties, so it acts as a SA to produce SLM operation in ring fiber lasers. The graphene SA suppresses multiple modes and reduces noise in the cavity. Graphene has the characteristics of saturation absorption. Therefore, in the case of low-intensity light irradiation, photons are highly absorbed, causing electrons in the valence band to be excited to the conduction band. When the intensity of irradiated light increases, a part of the photons are not absorbed due to the occupation of electrons in the conduction band, thereby allowing the light to pass through. Light will pass through the SA with low loss if it is high intensity light. The number of graphene layers is proportional to the light absorption rate, and each layer absorbs $A \approx 1\text{-}T \approx \pi \approx 2.3\%$ in the visible spectrum. As shown in **Figure 11**, the tuning range is 1,547–1,560 nm. Tunable fiber Bragg grating (TFBG) as a tuning element, and limited by the etching fineness.

Graphene has excellent thermal conductivity and ultra-high thermal conductivity, and has been widely used in tunable fiber lasers. The researchers used this characteristic of graphene to carry out temperature control tuning experiments, and achieved certain results.

Zhu Tao et al. realized an optically controlled ultra-narrow linewidth fiber laser [95]. This device uses saturable absorption

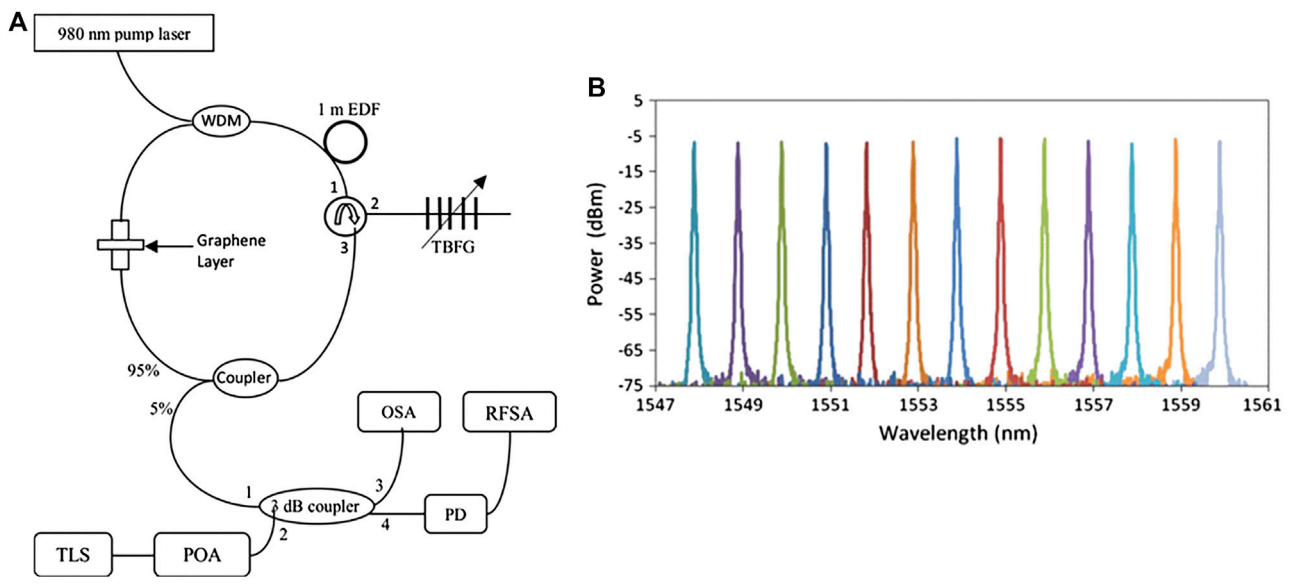

FIGURE 11 | (A) Experimental setup for tunable microwave generation by beating two SLM wavelengths from a tunable SLM ring fiber laser and external TLS. **(B)** Output spectra vs. wavelengths of the ring fiber laser. Copyright 2012, Optical Society of America.

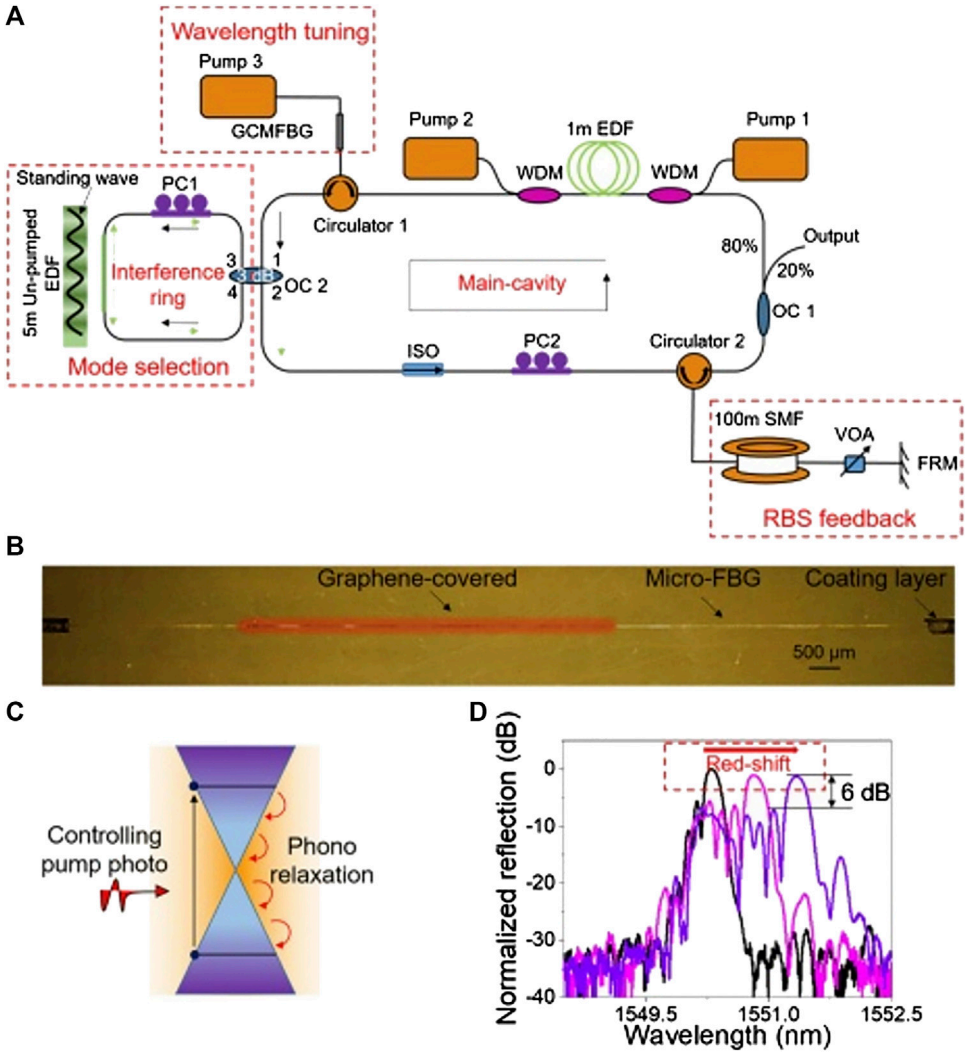

FIGURE 12 | (A) The setup of an optically tunable ultra-narrow linewidth fiber laser; **(B)** Photograph of a graphene-coated micro FBG (GCMFBG). The red shaded area is coated with graphene. **(C)** The phonon relaxation process of graphene; **(D)** The red-shifted reflection spectrum of GCMFBG, whose control optical power is 26.8, 64.3 and 101.5 mW. Copyright 2018, Optical Society of America.

interference ring and fiber Rayleigh backscatter (RBS) to compress linewidth and achieve mode selection. The interference loop is used as a narrow-band filter to enable the laser to achieve SF operation. Using graphene-covered ultra-fine fiber Bragg grating (GCMFBG), the laser wavelength can be precisely adjusted by controlling outpower. Finally, an output with a sensitivity of 12.4 pm/mW, a fluctuation in operating power of less than 0.5% and linewidth of 200 Hz was obtained [96–98]. The experimental setup is shown in **Figure 12A**.

In the experiment, a dual-pump structure was used, and a highly doped single-mode erbium-doped fiber with a length of 1 m was used in the cavity to provide gain. The output wavelength tuning operation of the laser is achieved by covering a single layer of graphene with a length of 12 mm miniature fiber Bragg grating (GCMFBG). When the pump light is absorbed by the graphene carrier, they will transition to the conduction band of zero band gap. Then they spontaneously fall to lower energy levels through phonon radiation to achieve self-heating [94]. Due to the high thermal conductivity of graphene, when increasing the control optical power, the miniature FBG is heated to achieve spectral wavelength shift, as shown in **Figure 12D**. The change in the refractive index of graphene affects the change in the effective refractive index of GCMFBG, which is another factor that changes the center wavelength of reflection. Tuning devices based on two-dimensional materials are different from the previous mechanical fine-tuning methods. They use the photothermal effect caused by the photo-excited interaction of carriers and phonons in graphene to achieve precise pump power tuning operations. Therefore, the tuning accuracy and stability are mainly controlled by the power of the pump light and the stability of the cavity. The tested wavelength and power stability are good under free operation. The

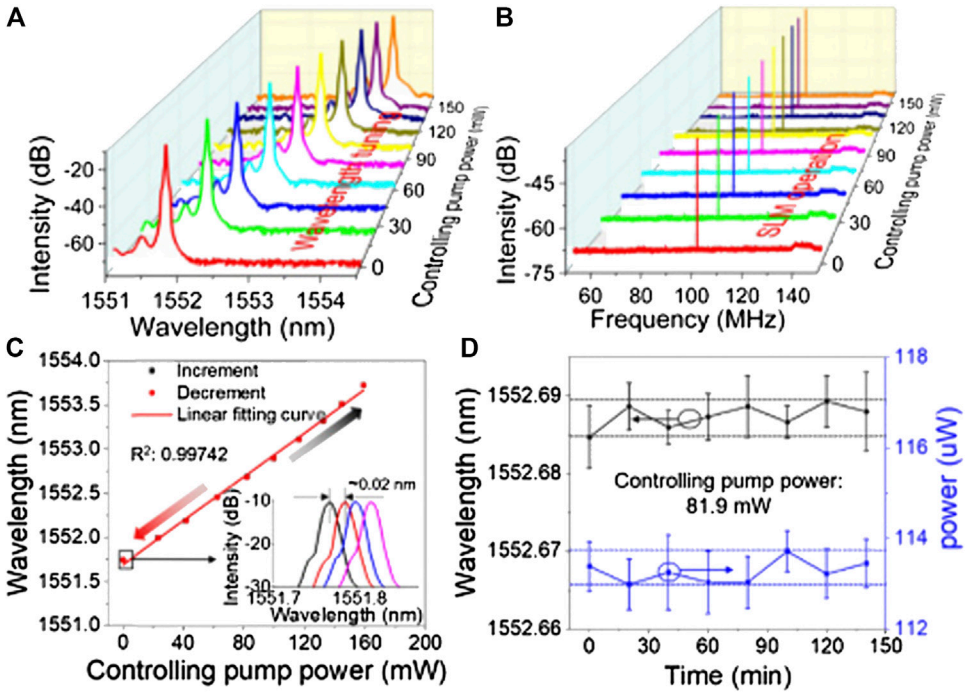

FIGURE 13 | (A) Output spectra of the ultra-narrow linewidth laser with the increment of the pump 3; **(B)** color-corresponded RF spectra during the tuning process; **(C)** peak wavelengths with changed powers of pump three and the linear fitting curve; **(D)** long-term stability test of the wavelength and output power with a fixed power of pump 3. Copyright 2018, Optical Society of America.

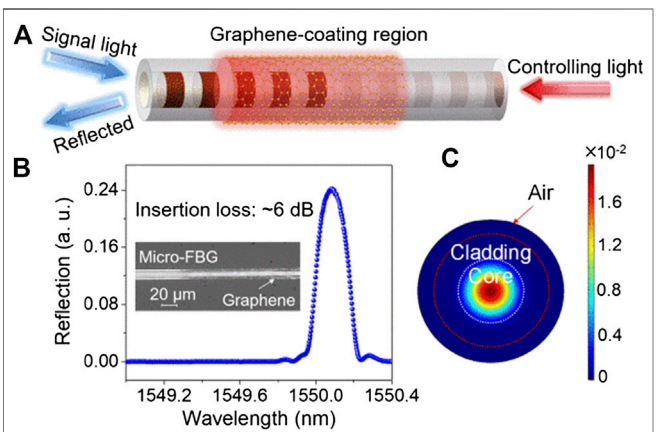

FIGURE 14 | (A) Experimental schematic of the fabricated GCMFBG and **(B)** its reflection spectrum; **(C)** circular symmetrical energy distribution of the controlling. Copyright 2019, Optical Society of America.

fluctuation ranges are 0.005 nm and 0.5%, respectively, and the operation is stable. The tuning characteristics are shown in **Figure 13**.

In 2019, Yujia Li et al. verified the use of graphene-coated filters using the narrow linewidth characteristics of Brillouin laser oscillations for SLM work. Tunable narrow-linewidth fiber lasers can be obtained with output linewidths as low as 750 Hz [99]. The laser wavelength can be linearly adjusted to 0.9997 by adjusting the laser with a wavelength of 13.2 pm/m, thereby adjusting the performance of the laser throughout the round trip. **Figure 14** shows the configuration of the light-controlled GCMFBG.

In this paper, the optically adjustable narrow linewidth fiber laser is wavelength tuned by a graphene-coated micro Bragg fiber grating (GCMFBG) module. Because graphene has broadband absorption properties, there is no special requirement to control the wavelength of light. The evanescent field of control light in contact with graphene stimulates graphene to easily produce photothermal effect to adjust the central reflection wavelength of GCMFBG. Insert GCMFBG into the fiber laser cavity to adjust the mode competition optically and achieve precise tunability of the laser wavelength. With low propagation loss and single-mode uniform distribution, stimulated Brillouin scattering (SBS) in the cavity can accumulate enough pump light intensity to be used as a narrow-band filter with a gain bandwidth of tens of megahertz [100, 101]. This optically tunable laser is used as pump light and injected into the polarization-maintaining cavity to excite SBS to achieve SLM operation and narrow linewidth laser output.

SUMMARY AND OUTLOOK

Wavelength tunable SF fiber lasers have important applications in many fields, such as spectral detection, laser radar, optical communication, fiber sensing, interferometer and so on. Considering the advantages of high stability, high linearity and high precision of optical control tuning, this fiber laser

has great application potential in the fields of microwave generation, high-precision sensing and optical communication. Due to the transmission of this tuning method, the idea of all-optical control can be further applied to other ultrafast laser systems, and is conducive to the development of laser miniaturization. In this review, the basic working principle and the latest development of wavelength tunable SF fiber lasers with 2D materials are summarized. As a new kind of materials, 2D materials have excellent performance in thermal, electrical and especially optical properties. In fiber lasers, on the one hand, the wide absorption spectrum of 2D materials and the excellent nonlinear saturable absorption effect increase the oscillation threshold of specific frequency in the cavity. Combined with filter components and frequency selective devices, the laser finally realizes the wavelength tunable SF operation; On the other hand, the excellent heat conduction characteristics of 2D materials can be used to achieve the wavelength selector by combing 2D materials with fiber Bragg grating, together with frequency filter, the operation of wavelength tunable SF operation can also be realized. Besides, 2D materials are also expected to achieve SF Q-switched pulse output considering the nonlinear saturable absorption. In addition, the excellent photoelectric characteristics of 2D materials can also be used to realize the photoelectric modulator, and it is expected that this kind of photoelectric modulator can be used in the fiber laser to realize mode-locking and Q-switched pulse output. There are some challenges in the application of 2D materials in the wavelength tunable SF fiber laser: 1) The existing technologies are difficult to obtain a large area of uniform materials; 2) The packaging technology needs to be improved to obtain more stable laser performance. 3) Two-dimensional materials are not abundant enough in the direction of single-frequency lasers. Further work in these directions will certainly promote the further development of optical fiber laser technology.

AUTHOR CONTRIBUTIONS

WZ finished writing the whole article. CS is responsible for part of the work. DJ completed part of the work of the single-frequency fiber laser. LB, QX, and SB is responsible for article modification.

ACKNOWLEDGMENTS

This work was supported by Open Research Fund of State Key Laboratory of Transient Optics and Photonics (SKLST201805).

REFERENCES

1. Xu M, Liang T, Shi M, Chen H. Graphene-Like two-dimensional materials. *Chem Rev* (2013) **113**:3766–98. doi:10.1021/cr300263a
2. Li XM, Yang HR, Cui YD, Chen GW, Yang Y, Tong LM. Graphene-clad microfibre saturable absorber for ultrafast fiber lasers. *Sci Rep* (2016) **6**:26024. doi:10.1038/srep26024
3. Song YW, Jang SY, Han WS, Bae MK. Graphene mode-lockers for fiber lasers functioned with evanescent field interaction. *Appl Phys Lett* (2010) **96**(5): 051122. doi:10.1063/1.3309669
4. Sun Z, Hasan T, Torrisi F, Popa D, Privitera G, Wang F, et al. Graphene mode-locked ultrafast laser. *ACS Nano* (2010) **4**:803. doi:10.1021/nn901703e
5. Cygan A, Lisak D, Morzyński P, Bober M, Zawada M, Pazderski E, et al. Cavity mode-width spectroscopy with widely tunable ultra narrow laser. *Opt Express* (2013) **21**(24):29744–54. doi:10.1364/oe.21.029744
6. Chang H, Fujiwara N, Watanabe K, Kanazawa S, Itoh M, Takenouchi H, et al. Narrow linewidth tunable DFB laser array integrated with optical feedback planar lightwave circuit (PLC). *IEEE J Sel Top Quant Electron* (2017) **23**(6): 1501007. doi:10.1109/jstqe.2017.2693021
7. Yeom H, Choi SY, Rotermund F, Lee K, Yeom D-I. All-polarization maintaining passively mode-locked fiber laser using evanescent field interaction with single-walled carbon nanotube saturable absorber. *J Lightwave Technol* (2016) **34**: 3510–4. doi:10.1109/jlt.2016.2543754
8. Koshikiya Y, Fan X, Ito F. Long range and cm-level spatial resolution measurement using coherent optical frequency domain reflectometry with SSB-SC modulator and narrow linewidth fiber laser. *J Lightwave Technol* (2008) **26**(18):3287–94. doi:10.1109/jlt.2008.928916
9. Li J, Gan J, Zhang Z, Heng X, Yang C, Qian Q, et al. High spatial resolution distributed fiber strain sensor based on phase-OFDR. *Optic Express* (2017) **25**(22):27913–22. doi:10.1364/oe.25.027913
10. Zhao LM, Tang DY, Zhang H, Wu X, Bao Q, Loh KP. Dissipative soliton operation of an ytterbium-doped fiber laser mode locked with atomic multilayer graphene. *Opt Lett* (2010) **35**(21):3622–4. doi:10.1364/ol.35.003622
11. Du WX, Li HP, Liu C, Shen SN, Lan CY, Li C, Liu Y. Ultrafast pulse erbium-doped fiber laser with a graphene/WS2 heterostructure saturable absorber. *Proc SPIE* (2017) **10457**:104571M. doi:10.1117/12.2284368
12. Ge Y, Chen S, Xu Y Z, Liang Z, Chen Y, et al. Few-layer selenium-doped black phosphorus: synthesis, nonlinear optical properties and ultrafast photonics applications. *J Mater Chem C* (2017) **5**(25):6129–35. C6NR09183K/c7tc01267e
13. He B, Wang S-H, Wu Z-X, Wang Z-X, Wang D-H, Hao H, et al. Sub-200 fs soliton mode-locked fiber laser based on bismuthene saturable absorber. *Opt Express* (2018) **26**:22750–60. doi:10.1364/oe.26.022750
14. Ko S, Lee J, Lee JH. Passively Q-switched ytterbium-doped fiber laser using the evanescent field interaction with bulk-like WTe2 particles. *Chin Opt Lett* (2018) **16**:020017. doi:10.3788/COL201816.020017
15. Li W, Zhu C, Rong X, Wu J, Xu H, Wang F, et al. Bidirectional red-light passively Q-Switched all-fiber ring lasers with carbon nanotube saturable absorber. *J Lightwave Technol* (2018) **36**:2694–701. doi:10.1109/jlt.2017.2781702
16. Liu J, Chen Y Y, Zhang H, Zheng S, Xu S. Dual-wavelength Q-switched fiber laser using multilayer black phosphorus as a saturable absorber. *Photon Res* (2018) **6**(3):198–203. doi:10.1364/prj.6.000198
17. Mao D, She XY, Du BB, Yang DX, Zhang WD, Song K, et al. Erbium-doped fiber laser passively mode locked with few-layer WSe2/MoSe2 nanosheets. *Sci Rep* (2016) **6**:23583. doi:10.1038/srep23583
18. Tang Z, Wang J, Yin J, Ouyang D, Ren X, Yan P, et al. High-power mode-locked thulium-doped fiber laser with tungsten ditelluride as saturable absorber. *Appl Opt* (2020) **59**:196–200. doi:10.1364/ao.59.000196
19. Ni SR. Graphene-based optoelectronics. *J Lightwave Technol* (2015) **33**(5): 1100–1108. doi:10.1109/JLT.2014.2373173
20. Bao Q, Zhang H, Ni Z, Wang Y, Polavarapu L, Shen Z, et al. Monolayer graphene as a saturable absorber in a mode-locked laser. *Nano Res* (2011) **4**(3): 297–307. doi:10.1007/s12274-010-0082-9
21. Zhang H, Tang DY, Knize RJ, Zhao L, Bao Q, Loh KP Graphene mode locked, wavelength-tunable, dissipative soliton fiber laser. *Appl Phys Lett* (2010) **96**(11):11112. doi:10.1063/1.3367743

22. David S, Rosa GH, Eunezio A. Influence of carbon nanotubes saturable absorbers diameter on mode-locking erbium-doped fiber laser performance. *J Lightwave Technol* (2017) **35**:4804–8. doi:10.1109/JLT.2017.2757951
23. Jeong H, Choi SY, Rotermund F, Lee K, Yeom D-I. All-polarization maintaining passively mode-locked fiber laser using evanescent field interaction with single-walled carbon nanotube saturable absorber. *J Lightwave Technol* (2016) **34**:3510–4. doi:10.1109/jlt.2016.2543754
24. Huang HY, Hou L, Wang Y, Sun J, Lin Q, Bai Y, et al. Tunable ytterbium-doped mode-locked fiber laser based on single-walled carbon nanotubes. *J Lightwave Technol* (2019) **37**(10):2370–74. doi:10.1109/jlt.2019.2904980
25. Harun XH, Wang Y-G, Wang Y-S, Hu X-H, Zhao W, Liu X-L, et al. Wavelength-switchable and wavelength-tunable all-normal-dispersion mode-locked Yb-doped fiber laser based on single-walled carbon nanotube wall paper absorber. *IEEE Photonics J* (2012) **4**(1):234–41. doi:10.1109/JPHOT.2012.2183862
26. Liu M, Liu W, Liu Z, Quhe RG, Lei M, Fang SB, et al. MoTe2 saturable absorber with high modulation depth for erbium-doped fiber laser. *J Lightwave Technol.*(2019) **37**(13):3100–5. doi:10.1109/jlt.2019.2910892
27. Wei M, Ou Y, Hou H, Liu W, Wei Z. Q-switched fiber laser operating at 1.5 μm based on WTe2. *China Optics Lett* (2019) **17**:020006. CNKI:SUN:GXKB.0.2019-02-006
28. Liu WJ, Liu ML, Liu B, Quhe RG, Lei M, Fang SB, et al. Nonlinear optical properties of MoS2-WS2 heterostructure in fiber lasers. *Opt Express* (2019) **27**:6689–99. doi:10.1364/oe.27.006689
29. Taylor SQ, Wang QK, Zhao CJ, Li Y, Zhang H, Wen S. Stable single-longitudinal-mode fiber ring laser using topological insulator-based saturable absorber. *J Lightwave Technol* (2014) **32**:3836–42. doi:10.1109/JLT.2014.2358855
30. Liu X, Guo Q, Qiu J. Emerging low-dimensional materials for nonlinear optics and ultrafast photonics. *Adv Mater* (2017) **29**:1605886. doi:10.1002/adma.201605886
31. Balandin AA, Ghosh S, Bao W, Calizo I, Teweldebrhan D, Miao F, Lau CN. Superior thermal conductivity of single-layer graphene. *Nano Lett* (2008) **8**(3):902–7. doi:10.1021/nl0731872
32. Yan PG. Large-area tungsten disulfide for ultrafast photonic. *Nanoscale* (2016) **9**:1871–77. C6NR09183K/C6NR09183K
33. Lu B, Yuan LM, Qi XY, Hou L, Sun B, Fu P, et al. MoS2 saturable absorber for single frequency oscillation of highly Yb-doped fiber laser. *Chin Optic Lett* (2016) **14**:5. doi:10.3788/COL201614.071404
34. Chen S, Wang QK, Zhao CJ, Li Y, Wen SC. Stable single-longitudinal-mode fiber ring laser using topological insulator-based saturable absorber. *J Lightwave Technol* (2014) **32**(22):4438–44.
35. Yao BC, Rao YJ, Huang SW, Wu Y, Feng ZY, Choi C, et al. Graphene Q-switched distributed feedback fiber lasers with narrow linewidth approaching the transform limit. *Opt Express* (2017) **25**(7):8202–11. doi:10.1364/OE.25.008202
36. Yin JJ, Luo A, Luo Z, Wang X, Feng X, Guan B-o. Dual-wavelength single-longitudinal-mode fiber laser with switchable wavelength spacing based on a graphene saturable absorber. *Photon Res* (2015) **3**(2):A21. doi:10.1364/prj.3.000a21
37. Muhammad FD, Zulkifli MZ, Latif AA, Harun SW, Ahmad H. Graphene-based saturable absorber for single-longitudinal-mode operation of highly doped erbium-doped fiber laser. *IEEE Photonics J* (2012) **4**:467–75. doi:10.1109/jphot.2012.2190498
38. Li H. Single frequency fiber laser based on ultrathin metal-organic framework. *J Mater Chem C* (2019) **16**(8):1822–4. doi:10.1039/C8TC03780A
39. Luo ZQ. 212-kHz-linewidth, transform-limited pulses from a single-frequency Q-switched fiber laser based on a few-layer Bi2Se3 saturable absorber. *Photon Res* (2018) **10**(6):C29–C35. doi:10.1364/PRJ.6.000C29
40. Li MZ, Muhammad FD, Mohd Azri MF, Mohd Yusof MK, Hamdan KZ, Samsudin SA, et al. Tunable passively Q-switched ultranarrow linewidth erbium-doped fiber laser. *Results in Physics* (2020) **16**:102949. doi:10.1016/j.rinp.2020.102949
41. Ball GA, Morey WW. Continuously tunable single-mode erbium fiber laser. *Opt Lett* (1992) **17**(6):420–2. doi:10.1364/ol.17.000420
42. Choma M, Sarunic M, Yang C, Izatt J. Sensitivity advantage of swept source and Fourier domain optical coherence tomography. *Opt Express* (2003) **11**(18):2183–9. doi:10.1364/oe.11.002183
43. Delgado-Pinar M, Mora J, Díez A, Cruz JL, Andrés MV. Wavelength-switchable fiber laser using acoustic waves. *IEEE Photon Technol Lett* (2005) **17**(3):552–4. doi:10.1109/lpt.2004.840021
44. Huang L, Song X, Chang P, Peng W, Zhang W, Gao F, et al. All-fiber tunable laser based on an acousto-optic tunable filter and a tapered fiber. *Optic Express* (2016) **24**(7):7449–55. doi:10.1364/oe.24.007449
45. Svelto AA, Zulkifli MZ, Awang NA, Harun SW, Ahmad H. A simple linear cavity dual-wavelength fiber laser using AWG as wavelength selective mechanism. *Laser Phys* (2010) **20**:2006–10. doi:10.1134/s1054660x10210061
46. Yin N, Wang L, Jain R. Single-longitudinal-mode tunable WDM-channel-selectable fiber laser. *Opt Express* (2002) **10**(25):1503–7. doi:10.1364/oe.10.001503
47. Maeda MW, Patel JS, Smith DA, Lin C, Saifi MA, Lehman AV. An electronically tunable fiber laser with a liquid-crystal etalon filter as the wavelength-tuning element. *IEEE Photon Technol Lett* (1990) **2**(11):787–9. doi:10.1109/68.63221
48. Pan S, Yao J. A wavelength-switchable single-longitudinal-mode dual-wavelength erbium-doped fiber laser for switchable microwave generation. *Opt Express* (2009) **17**:5414–9. doi:10.1364/oe.17.005414
49. Smith DA, Maeda MW, Johnson JJ, Patel JS, Saifi MA, von Lehman A. Acoustically tuned erbium-doped fiber ring laser. *Opt Lett* (1991) **16**(6):387–9. doi:10.1364/ol.16.000387
50. Song YW, Havstad SA, Starodubov D, Xie Y, Willner AE, Feinberg J. 40-nm-wide tunable fiber ring laser with single-mode operation using a highly stretchable FBG. *IEEE Photon Technol Lett* (2001) **13**(11):1167–9. doi:10.1109/68.959352
51. Song YW, Havstad SA, Starodubov D, Xie Y, Willner AE, Feinberg J. 40-nm-Wide tunable fiber ring laser with single-mode operation using a highly stretchable FBG. *IEEE Photon Technol Lett* (2001) **13**(11):1167–9. doi:10.1109/68.959352
52. Hotate JG, Sun JQ. Stable and widely tunable wavelength spacing single longitudinal mode dual-wave length erbium-doped fiber laser. *Opt Fiber Technol* (2010) **16**(4):299–303. doi:10.1016/j.yofte.2010.06.004
53. Chen N, Han X, Chang P, Huang L, Gao F, Yu X, et al. Tunable dual-wavelength fiber laser with unique gain system based on in-fiber acousto-optic Mach-Zehnder interferometer. *Opt Express* (2017) **25**(22):27609–15. doi:10.1364/oe.25.027609
54. Yao Y, Chen XF, Dai YT, Xie SZ. Dual-wavelength erbium-doped fiber laser with a simple linear cavity and its application in microwave generation. *IEEE Photon Technol Lett* (2006) **18**(1):187–9. doi:10.1109/LPT.2005.861309
55. Zhang J, Yue C, Schim G, Clements W, Lit J. Stable single-mode compound-ring erbium-doped fiber laser. *IEEE Photonics Technol Lett* (1996) **14**(1):104–9.
56. Ahmad H, bt Muhammad FD, Zulkifli MZ, Latif AA, Harun SW. Radio frequency generation using a graphene-based single longitudinal mode fiber laser. *J Lightwave Technol* (2012) **30**(13):2097–102. doi:10.1109/jlt.2012.2192099
57. Fang Q, Xu Y, Fu S, Shi W. Single-frequency distributed Bragg reflector Nd doped silica fiber laser at 930 nm. *Opt Lett* (2016) **41**(8):1829–32. doi:10.1364/ol.41.001829
58. Yang C, Chen D, Xu S, Deng H, Lin W, Zhao Q, et al. Short all Tm-doped germanate glass fiber MOPA single-frequency laser at 195 μm. *Optic Express* (2016) **24**(10):10956–10961. doi:10.1364/oe.24.010956
59. Yin B, Feng SC, Liu ZB, Bai YL, Jian SS. Single-frequency and single-polarization DFB fiber laser based on tapered FBG and self-injection locking. *IEEE Photonics J* (2015) **7**(3):1501909. doi:10.1109/jphot.2015.2426871
60. Feng S, Mao Q, Tian Y, Ma Y, Li W, Wei L. Widely tunable single longitudinal mode fiber laser with cascaded fiber-ring secondary cavity. *IEEE Photon Technol Lett* (2013) **25**(4):323–6. doi:10.1109/lpt.2012.2235141
61. Li B, Wei X, Wang X, Wong KK-Y. Single-longitudinal-mode Brillouin/erbium fiber laser with high linewidth-reduction ratio. *IEEE Photon Technol Lett* (2014) **26**(23):2387–90. doi:10.1109/lpt.2014.2357831

62. Lim SD, Yoo JK, Kim SK. Widely tunable watt-level single-frequency Tm-doped fiber ring laser as pump for Mid-IR frequency generation. *IEEE Photonics J* (2016) **8**(3):1502006. doi:10.1109/jphot.2016.2574358
63. Muhammad FD, Zulkifli MZ, Latif AA, Harun SW, Ahmad H. Graphene-based saturable absorber for single-longitudinal-mode operation of highly doped erbium-doped fiber laser. *IEEE Photonics J* (2012) **4**(2):467–75. doi:10.1109/jphot.2012.2190498
64. Yang W, Lu P, Wang S, Liu D, Zhang J, Chen E, et al. A novel switchable and tunable dual-wavelength single-longitudinal-mode fiber laser at 2. *IEEE Photon Technol Lett* (2016) **28**(11):1161–1164. doi:10.1109/lpt.2016.2528039
65. Yeh CH, Chen JY, Chen HZ, Chen JH, Chow CW. Stable and tunable single-longitudinal-mode erbium-doped fiber triple-ring laser with power-equalized output. *IEEE Photonics J* (2016) **8**(2):1500906. doi:10.1109/jphot.2016.2539551
66. Zhang L, Zhan L, Qin M, Zou Z, Wang Z, Liu J. Large-region tunable optical bistability in saturable absorber-based single-frequency Brillouin fiber lasers. *J Opt Soc Am B* (2015) **32**(6):1113–9. doi:10.1364/josab.32.001113
67. Choma M, Sarunic M, Yang C, Izatt J. Sensitivity advantage of swept source and Fourier domain optical coherence tomography. *Opt Express* (2003) **11**(18):2183–9. doi:10.1364/oe.11.002183
68. Jauncey IM, Reekie L, Mears RJ, Payne DN, Rowe CJ, Reid DCJ, et al. Narrow-linewidth fibre laser with integral fibre grating. *Electron Lett* (2007) **22**(19):987–8. doi:10.1049/el:19860675
69. Tang J, Sun J. Stable and widely tunable wavelength-spacing single longitudinal mode dual-wavelength erbium-doped fiber laser. *Opt Fiber Technol* (2010) **16**:299–303. doi:10.1016/j.yofte.2010.06.004
70. Zhu C, Zhang B, Shi L, Huang C, Deng M, Liu J, et al. Tunable dual-wavelength fiber laser with ultra-narrow linewidth based on Rayleigh backscattering. *Optic Express* (2016) **24**(2):1324–30. doi:10.1364/oe.24.001324
71. Iwatsuki K, Okamura H, Saruwatari M. Wavelength-tunable single-frequency and single-polarisation er-doped fibre ring-laser with 1.4 kHz linewidth. *Electron Lett* (1990) **26**(24):2033–5. doi:10.1049/el:19901312
72. Latif GA, Morey WW. Standing wave mono-mode erbium fiber laser. *IEEE Photon Technol Lett* (1991) **3**(7):613–5. doi:10.1109/68.87930
73. Bonaccorso F, Sun Z, Hasan T, Ferrari AC. Graphene photonics and optoelectronics. *Nat Photon* (2010) **4**:611–22. doi:10.1038/nphoton.2010.186
74. Fu S, Shi W, Sheng Q, Shi G, Zhang H, Yao J. Extended linear cavity 2 u m single-frequency fiber laser using Tm-doped fiber saturable absorber. Conference on lasers and electro-optics; 14–19 May 2017; San Jose, CA, Optical Society of America (2017)
75. Guy MJ, Taylor JR, Kashyap R. Single-frequency erbium fibre ring laser with intracavity phase-shifted fibre Bragg grating narrowband filter. *Electron Lett* (1995) **31**(22):1924–5. doi:10.1049/el:19951297
76. He X, Xu S, Li C, Yang C, Yang Q, Mo S, et al. 195 μm kHz-linewidth single-frequency fiber laser using self-developed heavily Tm^3+-doped germanate glass fiber. *Optic Express* (2013) **21**(18):20800. doi:10.1364/oe.21.020800
77. Yang M, Zyskind J, Daisy R, Fischer B. Narrow-linewidth, singlemode erbium-doped fibre laser with intracavity wave mixing in saturable absorber. *Electron Lett* (1994) **30**(8):648–9. doi:10.1049/el:19940448
78. Yeom Y, Spiegelberg C, Geng J, et al. 200-mW, narrow—linewidth 1 064. 2-am Yb-doped fiber laser. Lasers and Electro-optics. (2004)
79. Kishi N, Yazaki T. Frequency control of a single-frequency fiber laser by cooperatively induced spatial-hole burning. *IEEE Photon Technol Lett* (1999) **11**(2):182–4. doi:10.1109/68.740697
80. Kringlebotn JT, Morkel PR, Reekie L, Archambault J-L, Payne DN. Efficient diode-pumped single-frequency erbium: ytterbium fiber laser. *IEEE Photon Technol Lett* (1993) **5**(10):1162–64. doi:10.1109/68.248414
81. Kringlebotn JT, Archambault J-L, Reekie L, Laming RI, Payne DN. Nd:YLF pumped grating-feedback Er^{3+}:Yb^{3+}Co-doped silica fiber laser operating at 1.49 μm. *Opt Fiber Technol* (1996) **2**:69–74. doi:10.1006/ofte.1996.0006
82. Laming P, Longh S, Taccheo S, Svelto O, Sacchi G. 10 kHz-linewidth diode-pumped Er:Yb:glass laser. *Electron Lett* (1992) **28**(22):2067–9. doi:10.1049/el:19921325
83. Park N, Dawson JW, Vahala KJ, Miller C. All fiber, low threshold, widely tunable single-frequency, erbium-doped fiber ring laser with a tandem fiber Fabry-Perot filter. *Appl Phys Lett* (1991) **59**(19):2369. doi:10.1063/1.106018
84. Takushima Y, Yamashita S, Kikuchi K, Hotate K. Polarization-stable and single-frequency fiber lasers. *J Lightwave Technol* (1998) **16**(4):661–9. doi:10.1109/50.664080
85. Wang T, Zhang L, Feng C, Qin M, Zhan L. Tunable bistability in hybrid Brillouin-erbium single-frequency fiber laser with saturable absorber. *J Opt Soc Am B* (2016) **33**(8):1635–9. doi:10.1364/josab.33.001635
86. Qin S, Yang Z, Zhang W, Wei X, Qian Q, Chen D, et al. 400 mW ultrashort cavity low-noise single frequency Yb3+-doped phosphate fiber laser. *Opt Lett* (2011) **36**(18):3708–10. doi:10.1364/OL.36.003708
87. Zhang Y, Zhang Y, Zhao Q, Li C, Yang C, Feng Z, et al. Ultra-narrow linewidth full C-band tunable single-frequency linear-polarization fiber laser. *Optic Express* (2016) **24**(23):26209. doi:10.1364/oe.24.026209
88. Li X, Li J, Zhou X, Ma Y, Zheng Z, Duan X, et al. Silver nanoparticles protected by monolayer graphene as a stabilized substrate for surface enhanced Raman spectroscopy. *Carbon* (2014) **66**:713–9. doi:10.1016/j.carbon.2013.09.076
89. Novoselov KS, Geim AK, Morozov SV, Jiang D, Zhang Y, Dubonos SV, et al. Electric field effect in atomically thin carbon films. *Science* (2004) **306**:666–9. doi:10.1126/science.1102896
90. Malard LM, Pimenta MA, Dresselhaus G, Dresselhaus MS. Raman spectroscopy in graphene. *Phys Rep* (2009) **473**:51–87. doi:10.1016/j.physrep.2009.02.003
91. Lin W, Duan X, Cui Z, Yao B, Dai T, Li X. A passively Q-switched Ho:YVO4 laser at 2.05 μm with graphene saturable absorber. *Appl Sci* (2016) **6**:128. doi:10.3390/app6050128
92. Bonaccorso F, Sun Z, Hasan T, Ferrari AC. Graphene photonics and optoelectronics. *Nat Photon* (2010) **4**:611–22. doi:10.1038/nphoton.2010.186
93. Balandin AA, Ghosh S, Bao W, Calizo I, Teweldebrhan D, Miao F, Lau CN. Superior thermal conductivity of single-layer graphene. *Nano Lett* (2008) **8**(3):902–7. doi:10.1021/nl0731872
94. Ahmad H, bt Muhammad FD, Zulkifli MZ, Latif AA, Harun SW. Radio frequency generation using a graphene-based single longitudinal mode fiber laser. *J Lightwave Technol* (2012) **30**(13):2097–102. doi:10.1109/jlt.2012.2192099
95. Wu Y, Huang L, Gao L, Lan T, Cao Y, Ikechukwu IP, et al. Optically controlled tunable ultra-narrow linewidth fiber laser with Rayleigh backscattering and saturable absorption ring. *Optic Express* (2018) **26**(21):26896–906. doi:10.1364/oe.26.026896
96. Chen M, Meng Z, Wang J, Chen W. Ultra-narrow linewidth measurement based on voigt profile fitting. *Optic Express* (2015) **23**(5):6803–8. doi:10.1364/oe.23.006803
97. Quhe O, Merrer PH, Brahimi H, Saleh K, Lacroix P. Phase noise measurement of a narrow linewidth CW laser using delay line approaches. *Opt Lett* (2011) **36**(14):2713–5. doi:10.1364/ol.36.002713
98. Vahala LE, Kruger HIS, Mcgrath PA. Linewidth determination from self-heterodyne measurement with sucoherence delay times. *Quan Electron Lett* (1986) **22**(11):2070–4.
99. Song YW, Havstad SA, Starodubov D, Xie Y, Willner AE, Feinberg J. 40-nm-Wide tunable fiber ring laser with single-mode operation using a highly stretchable FBG. *IEEE Photon Technol Lett* (2001) **13**(11):1167–9. doi:10.1109/68.959352
100. Debut A, Randoux S, Zemmouri J. Linewidth narrowing in brillouinlasers: theoretical analysis. *Phys Rev* (2000) **62**:578–92. doi:10.1103/physreva.62.023803
101. Huang S, Zhu T, Yin G, Lan T, Huang L, Li F, et al. Tens of hertz narrow-linewidth laser based on stimulated Brillouin and Rayleigh scattering. *Opt Lett* (2017) **42**(24):5286–5289. doi:10.1364/ol.42.005286

Conflict of Interest: The authors declare that the research was conducted in the absence of any commercial or financial relationships that could be construed as a potential conflict of interest